MCHPES 205 (8)
1001–1136

ISSN 1022–1352

D 51046

Vol. 205
May 21, 2004

8

Macromolecular Chemistry and Physics

www.mcp-journal.de

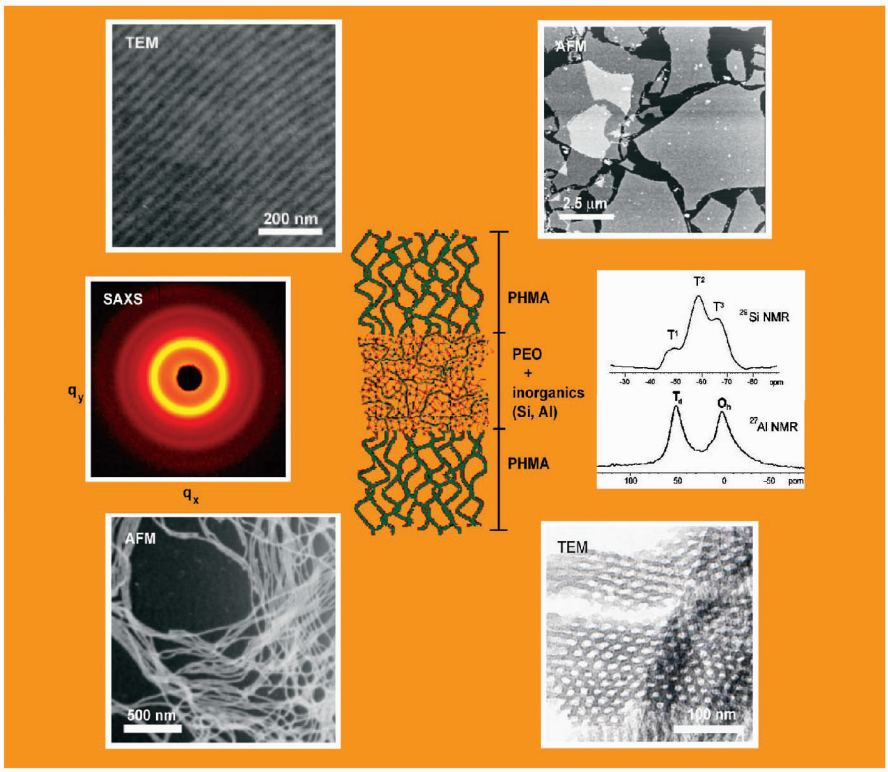

Founded by Hermann Staudinger

WILEY-VCH

Summary: The present study describes the use of poly(ethylene oxide)-*block*-poly(hexyl methacrylate) diblock copolymers (PEO-*b*-PHMA) as structure-directing agents for the synthesis of nanostructured polymer-inorganic hybrid materials from (3-glycidylpropyl)trimethoxysilane and aluminium *sec*-butoxide as precursors and organic, volatile solvents. Four different morphologies, i.e., inorganic spheres, cylinders, lamellae, and organic cylinders in an inorganic matrix, are obtained confirmed by a combination of small-angle X-ray scattering (SAXS) and transmission electron microscopy (TEM). The composites are further characterized by differential scanning calorimetry (DSC) and solid-state ^{13}C, ^{29}Si, and ^{27}Al NMR. It is demonstrated that the change in the hydrophobic block from polyisoprene (PI) to poly(hexyl methacrylate) (PHMA) has no significant effect on the local structure of the inorganic rich phase. By the dissolution of the composites rich in poly(hexyl methacrylate), nano-particles of different shapes, i.e., spheres, cylinders, and lamellae, are obtained as demonstrated by atomic force microscopy (AFM) and TEM. Finally, calcination of composites with the inverse hexagonal structure at elevated temperatures up to 600 °C results in nanostructured aluminosilicates that retain their structure as evidenced through a combination of SAXS and TEM. The study opens pathways towards tailoring filler-matrix interactions in model nanocomposites and builds the bases for the preparation of composites from multiblock copolymers with polyisoprene (PI), poly(ethylene oxide) (PEO), and poly(hexyl methacrylate) (PHMA) as building blocks.

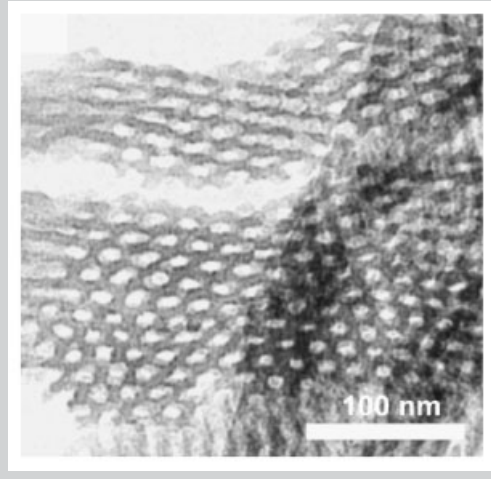

Bright field TEM micrograph of composite T55/1 with inverse hexagonal morphology after calcination.

Nanostructure and Shape Control in Polymer-Ceramic Hybrids from Poly(ethylene oxide)-*block*-Poly(hexyl methacrylate) and Aluminosilicates Derived from Them

Sabine Renker,[1a] *Surbhi Mahajan,*[2a] *Diane T. Babski,*[1] *Ingo Schnell,*[1] *Anurag Jain,*[2] *Jochen Gutmann,*[1] *Yuangming Zhang,*[2] *Sol M. Gruner,*[3] *Hans W. Spiess,*[1] *Ulrich Wiesner**[2]

[1] Max Planck Institute for Polymer Research, Ackermannweg 10, 55128 Mainz, Germany
[2] Department of Materials Science and Engineering, Bard Hall, Cornell University, Ithaca, NY 14853, USA
E-mail: ubw1@cornell.edu
[3] Department of Physics, Clark Hall, Cornell University, Ithaca, NY 14853, USA

Received: December 21, 2003; Revised: March 5, 2004; Accepted: March 11, 2004; DOI: 10.1002/macp.200300249

Keywords: amphiphiles; block copolymers; morphology; nanocomposites; structure-directing agent

Introduction

The study of amphiphilic block copolymer-derived, organic-inorganic hybrid materials is an emerging research field offering enormous scientific and technological potential. Amphiphiles, like polyisoprene-*block*-poly(ethylene oxide),[1] polybutadiene-*block*-poly(ethylene oxide),[2] polystyrene-*block*-poly(ethylene oxide),[3,4] poly(ethylene oxide)-*block*-poly(propylene oxide)-*block*-poly(ethylene oxide)[5] and alkyl-PEO alcohols,[6] have been used in conjunction with ceramic precursors in sol-gel processes to obtain arrays of nanocomposite morphologies. These composites can subsequently be employed to generate, e.g., mesoporous materials or nanoparticles of different shapes and sizes.[7]

[a] Both authors contributed equally to the paper.

 DOI: 10.1002/macp.200300249

In previous studies, we developed hybrid materials based on PI-*b*-PEO mixed in organic volatile solvents with the metal alkoxides, (3-glycidylpropyl)trimethoxysilane and aluminium *sec*-butoxide, in a sol-gel approach.[7] The metal alkoxides selectively swelled the PEO phase of the block copolymer due to the hydrophilic nature of PEO. The aluminium alkoxide served as a hardening component.[8] A range of morphologies were formed (Figure 1 shows a specific subset) by varying the polymer to metal alkoxides ratio demonstrating that the amphiphilic block copolymer PI-*b*-PEO functions as an effective structure-directing agent in the synthesis of structured organic-inorganic hybrid materials. So far, spherical, hexagonal and lamellar structures, the respective inverse phases, a wormlike micelle morphology and the so-called Plumber's Nightmare structure have been found for our system.[7,9,10] To obtain more complex hybrid structures, one strategy is to move from the phase behavior of diblock copolymers like PI-*b*-PEO to that of tri- or multiblock copolymers.[11–16] This should access a whole range of new morphologies to the design of polymer-inorganic hybrid materials.

The first step in this direction is the extension of the described hybrid synthesis to other amphiphilic, but chemically different diblock copolymers, which later can be combined with the PI-*b*-PEO base system. A suitable material, which could be used in the same way as PI-*b*-PEO, has to meet the following criteria: First, the building blocks should show phase separation at ambient temperatures. Second, the hydrolysis products of the metal alkoxides should preferentially swell the hydrophilic block. Third, a low glass transition temperature, T_g, of the hydrophobic block should introduce high mobility at ambient temperatures and should allow rapid formation of structures with long range order even in the bulk.

One candidate which fulfills all these requirements is the amphiphilic block copolymer, poly(ethylene oxide)-*block*-poly(hexyl methacrylate) PEO-*b*-PHMA. While the hydrophilic PEO block is maintained, the hydrophobic PI block is exchanged for poly(hexyl methacrylate), PHMA. The glass transition temperature of the PHMA block (approx. 268 K) should be low enough to guarantee high mobility during hybrid film formation. The synthesis of PEO-*b*-PHMA block copolymers by a combination of anionic polymerization and ATRP has been described in a recent publication.[17] Here, we show first results on the synthesis of hybrid materials casted from organic solvents derived from PEO-*b*-PHMA block copolymers and the metal alkoxides, (3-glycidylpropyl)trimethoxysilane and aluminium *sec*-butoxide.

Experimental Part

Materials

Chloroform ($CHCl_3$), tetrahydrofuran (THF), aluminium *sec*-butoxide (Fluka), (3-glycidylpropyl)trimethoxysilane (GLYMO, ABCR), and potassium chloride (KCl) were used

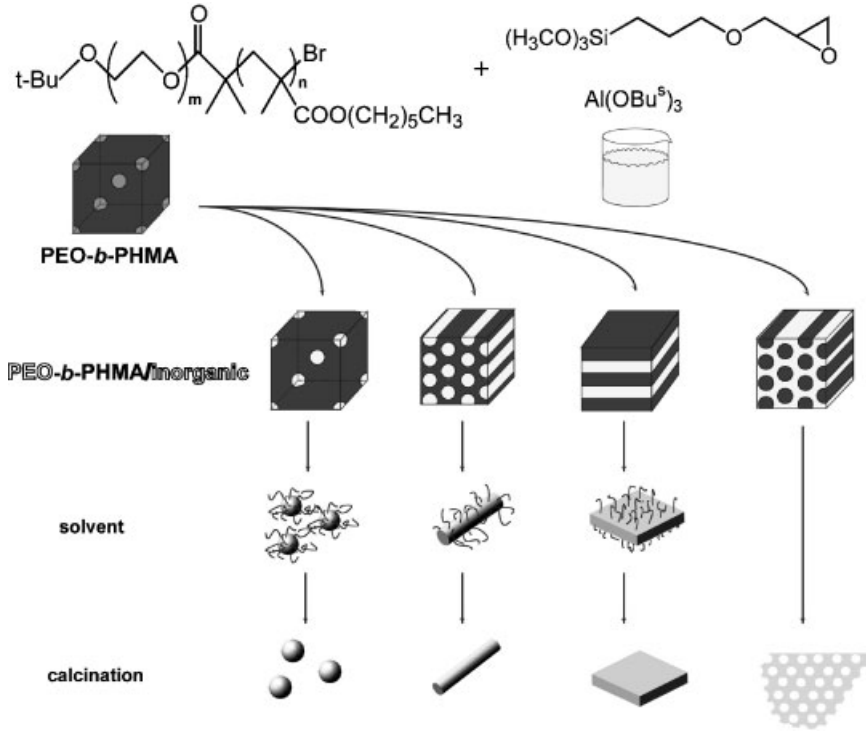

Figure 1. PEO-*b*-PHMA as structure-directing agent.

as received. The poly(ethylene oxide)-*block*-poly(hexyl methacrylate) copolymers (PEO-*b*-PHMA) were synthesized from commercial ethylene oxide (Fluka) and hexyl methacrylate (Aldrich) according to a recently published polymerization procedure.[17] Three different polymers were used to prepare the hybrids studied in this paper, referred to as T273 ($\overline{M}_n =$ 21 800 g/mol, $\overline{M}_w/\overline{M}_n = 1.19$, PEO weight fraction: 12%), T55 ($\overline{M}_n = 20\,960$ g/mol, $\overline{M}_w/\overline{M}_n = 1.16$, PEO weight fraction: 13%) and T37 ($\overline{M}_n = 18\,750$ g/mol, $\overline{M}_w/\overline{M}_n = 1.09$, PEO weight fraction: 16%). The morphology of these block copolymers in the bulk is a lattice of PEO spheres in a PHMA matrix as expected from diblock copolymer phase diagrams.

Characterization

For the characterization of the hybrid materials, small-angle X-ray scattering (SAXS) and transmission electron microscopy (TEM) were used. The SAXS setup consisted of a Rigaku rotating anode X-ray source (Cu K_α, $\lambda = 1.54$ Å), typically operated at 40 kV, 50 mA (Figure 2A, 2B and 2C). The X-rays were nearly monochromatized by Ni filtering followed by focusing onto the detector using a pair of crossed Franks mirrors. A two-dimensional CCD detector[18] (512 × 512 pixels) at a typical sample to detector distance of 60 cm was used to record the diffraction patterns. The powder pattern rings were azimuthally integrated around the incident beam direction to yield one-dimensional traces of diffracted intensity vs $q = 4\pi \sin\theta/\lambda$ where 2θ is the angle between the incident and scattered beam directions. These traces were divided by q to normalize to X-rays per unit area in the detector plane.

For Figure 2D and 11A, SAXS experiments were performed on a Bruker-AXS NanoSTAR. The setup consisted of an X-ray source (Cu K_α, 1.54 Å) operated at 40 kV and 40 mA. Göebbel mirrors were used to focus the beam. A 2-D Hi-Star arial detector at a sample to detector distance of 62.5 cm was used to record the scattering images. 2-D images were integrated over the azimuthal angle ϕ to obtain one dimensional intensity vs scattering plots.

A Zeiss EM 902 electron microscope operated at 80 kV using an objective aperture of 8 mrad was used to take the dark field images. Ultrathin sections were produced using a Leichert ultramicrotome. Bright field transmission electron micrographs were measured on a JEOL 1200EX operating at 120 kV.

Glass transition temperatures were measured by differential scanning calorimetry (DSC) on a Mettler DSC-30 over the temperature range −120 to 150 °C with a heating rate of 10 °C/min.

One-dimensional ^{27}Al magic-angle spinning (MAS) and ^{1}H-to-^{29}Si cross-polarization (CP) MAS NMR spectra were recorded on a Bruker ASX-500 spectrometer with a ^{1}H frequency of 500.1 MHz, an ^{27}Al frequency of 130.3 MHz, and a ^{29}Si frequency of 99.4 MHz. The alumina spectra were recorded at spinning speeds of 8 kHz using a small tip angle pulse (1 µs for $\gamma B_1/2\pi = 42$ kHz) and a recycle delay of 100 ms. For the ^{1}H-to-^{29}Si CP-MAS experiments, the 90° pulse length was 5 µs, the contact time was 2 ms, the recycle delay was 2 s, and the spinning speed was 4 kHz. Peak intensities were fitted using a deconvolution routine provided with the spectrometer software. ^{1}H-to-^{13}C CP-MAS experiments were also performed on this spectrometer. The ^{1}H Larmor frequency was 500.1 MHz, and the ^{13}C Larmor frequency was 125 MHz. The cross-polarization contact time was 2 ms, and the spinning

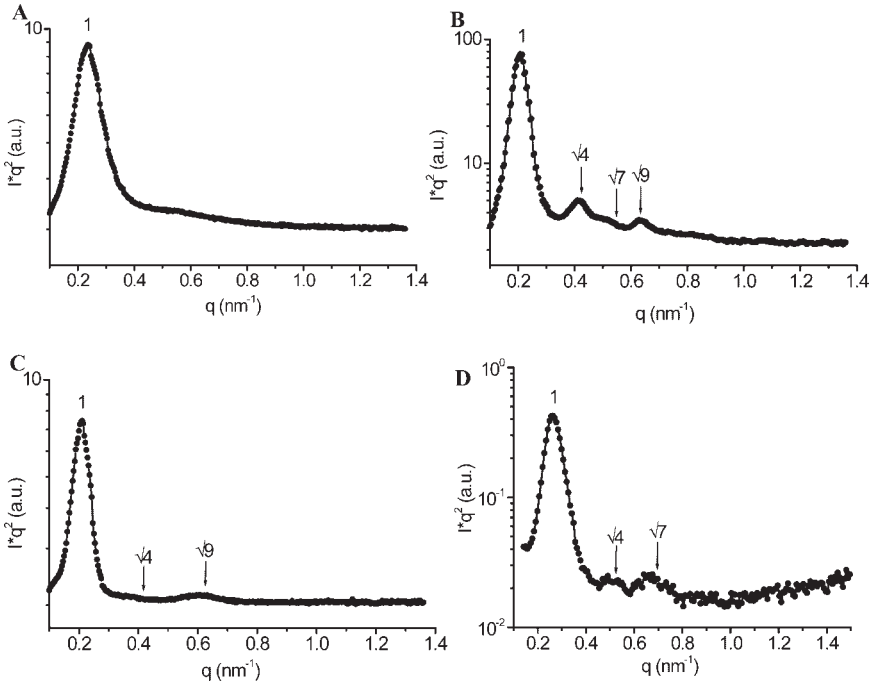

Figure 2. SAXS diffractograms of organic-inorganic hybrid materials with A) T273/1, 21 wt.-%, B) T273/2, 38 wt.-%, C) T273/3, 52 wt.-%, and D) T55/1, 69 wt.-% metal alkoxides in the hybrid material.

speed was 4 kHz. Recycle delays for the ^{1}H-to-^{13}C CP/MAS experiments were 2 s.

Atomic force microscopy samples were prepared by dip coating mica substrate in dilute solutions of nano-objects in toluene. The images were taken using a Veeco Nanoscope III Multimode scanning probe microscope employing tapping mode etched silicon tips.

Results and Discussion

Morphological Investigation

The ability of the PEO-*b*-PHMA block copolymer to act as a structure-directing agent in the synthesis of organic-inorganic hybrid materials was studied by mixing various amounts of a prehydrolyzed solution of (3-glycidyloxypropyl)trimethoxysilane (GLYMO) and aluminium *sec*-butoxide in a solution of PEO-*b*-PHMA block copolymers, T273, T55 or T37, in THF/$CHCl_3$. The molecular weights of the polymers varied between 18–22 kg/mol, the polydispersities were low ($\overline{M}_w/\overline{M}_n < 1.2$, where $\overline{M}_w$ and $\overline{M}_n$ are the weight-average and number-average molecular weights) and the weight fraction of the PEO block varied between 12 and 16%. After evaporation of the solvents at 50 °C and final condensation at 130 °C, clear, transparent hybrid films were obtained.

The morphologies of the resulting hybrid materials were studied by SAXS and TEM. Representative SAXS patterns from samples with 21, 38, 52, and 69% of metal oxides in the hybrid material, denoted as T273/1, T273/2, T273/3 and T55/1 (Table 1), are shown in Figure 2. For the hybrid with 21% aluminosilicate (T273/1, Figure 2A), no higher order peaks were found. For the hybrid material T273/2 with 38% aluminosilicate (Figure 2B), the spacing sequence is consistent with a hexagonal morphology. For the material with 52% aluminosilicate (T273/3, Figure 2C), a main peak and one reflection of higher order is clearly visible at multiples of the q value of the main peak. Such a sequence is characteristic of an arrangement of lamellae. When the aluminosilicate content is raised to 69% (T55/1, Figure 2D) reflections consistent with a hexagonal morphology were found.

Although the SAXS data are indicative, there were too few X-ray reflections to make unambiguous structure assignments. Therefore, TEM investigations were performed on all materials. The results are shown in Figure 3. The TEM images of composites T273/1 (Figure 3A), T273/2 (Figure 3B), T273/3 (Figure 3C) and T55/1 (Figure 3D) show spheres, cylinders (head-on), lamellae (side-on), and the inverse cylinder morphology (head-on), respectively, consistent with the SAXS results.

These results clearly demonstrate that the PEO-*b*-PHMA block copolymer is an effective structure-directing agent in the formation of structured organic-inorganic hybrid materials. As shown in Table 1, the correlations between composition and morphology for this composite system are consistent with those for the hybrids derived from PI-*b*-PEO described in earlier studies. This demonstrates the robustness of the present structure-directing approach. Besides the morphological characterization, it is interesting to look at the microstructure of the present hybrids. Indirect information about local structure is provided by differential scanning calorimetry (DSC). Figure 4 shows DSC plots for the pure block copolymer (T273, Figure 4A) as well as the spherical (T273/1, Figure 4B) and the hexagonal (T273/2, Figure 4C) hybrid materials derived from it. First, the crystallization behavior of the PEO phase is very different in the hybrids as compared to that in the bulk block copolymer. Whereas the pure block copolymer shows a strong melting peak at 36 °C (Figure 4A), crystallization of PEO is suppressed in the hybrids, providing evidence for co-localization of the inorganic and PEO phases. Residual melting is still observed for the composite with 21% aluminosilicate (Figure 4B), but crystallization is completely

Table 1. Different hybrid samples prepared from three PEO-*b*-PHMA block copolymers using various amounts of metal alkoxides and comparison with PI-*b*-PEO system.

Sample	Amount of metal alkoxide used[a)]	PEO + inorganic[b)]	Mesostructure	PEO + inorganic for system PI-*b*-PEO[c)]
	wt.-%	vol.-%		vol.-%
T273/1	21	24	spherical	23
T37/7	21	27	micelles	
T37/1	34	37	cylinders	28–32
T273/2	38	37		
T273/3	52	50	lamellae	45–53
T37/8	53	52		
T55/1	69	66	inverse cylinders	65–74

[a)] Wt.-% metal alkoxides based on the amount of material remaining after evaporation of all the volatile components (estimated to be 55% of initial weight of the sol).
[b)] Vol.-% (PEO + inorganic) were calculated using a density of 1.4 g/cm^3, see ref.[21]
[c)] From ref.[21]

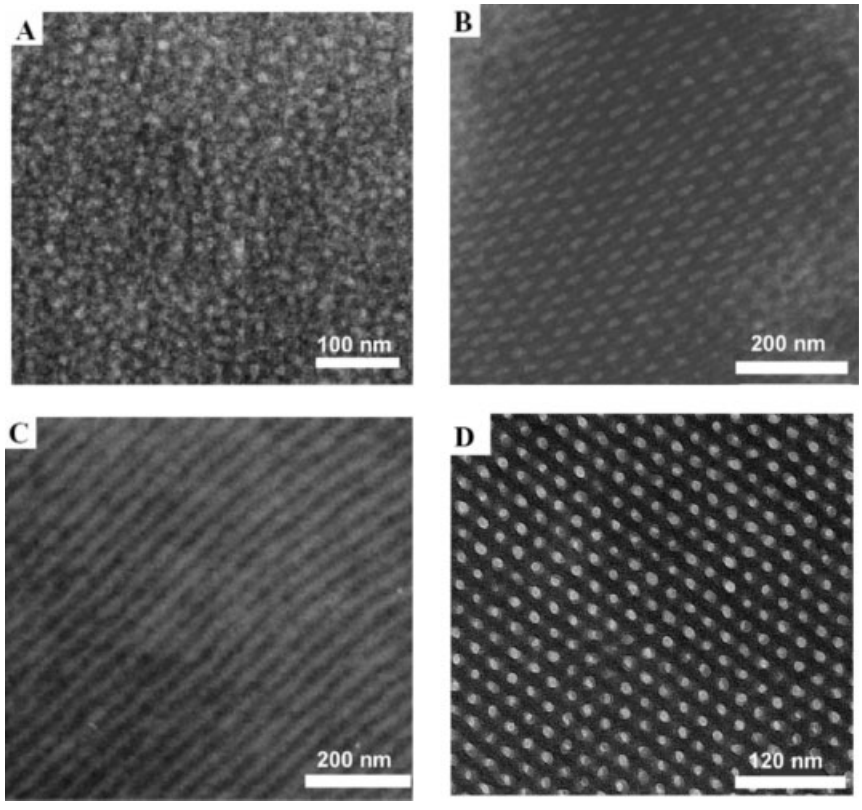

Figure 3. Dark field TEM micrographs of hybrid materials with A) T273/1, 21 wt.-%, B) T273/2, 38 wt.-% and C) T273/3, 52 wt.-% metal alkoxides. Under dark field conditions, the silicon and aluminium containing phase appears bright. Bright field TEM micrograph of hybrid material with D) T55/1, 69 wt.-% metal alkoxides (the PHMA phase appears bright).

suppressed in all hybrids with higher inorganic content PEO (Figure 4C). Furthermore, in the case of pure block copolymer (Figure 4A) and composite T273/1 (Figure 4B), a clear step in the DSC trace is observed around $-60\,^{\circ}C$ indicating the glass transition of amorphous PEO. Although the onset of a continuous change in slope is observed around this temperature for the composite T273/2 (Figure 4C), a well-developed step in the DSC trace cannot be identified. Consistent with the crystallization behavior this suggests that in composites with >21 wt.-% metal alkoxides, PEO is fully integrated into the inorganic network and significantly immobilized compared to amorphous bulk PEO. Finally, a step in the DSC trace around $-5\,^{\circ}C$ is observed for both composites indicating the glass transition, T_g, of amorphous PHMA, which is not affected by the presence of the inorganic network. In the pure block copolymer, the PHMA T_g is masked by the strong PEO melting peak.

Structural Investigation by Solid-State NMR

A deeper insight into the microstructure and the inorganic connectivities of the present hybrids could be gained by solid-state NMR. For the characterization of the organic groups, ^{13}C NMR was used. Figure 5 shows the ^{1}H-^{13}C CP-MAS NMR spectra of the pure PEO-*b*-PHMA block copolymer, T273, and its composite, T273/2, with lamellar morphology along with the peak assignments. Areas where significant spectral changes occur when going from block copolymer to composite are highlighted (Figure 5). The peak at $\sim$68 ppm (Figure 5B) is due to carbons adjacent to oxygen, which are present in PEO and GLYMO. This peak is significantly broader in the composite than in pure PEO-*b*-PHMA (Figure 5A) due to the structural disorder and rigidity in the aluminosilicate phase of the hybrid material. The aliphatic carbon atoms in GLYMO also give rise to relatively broad peaks at around 7 and 22 ppm. Different morphologies of the composites did not lead to significant spectral changes. This is not surprising since the local environments of the carbons, which are probed by the chemical shift, are not expected to differ in kind from sample to sample.

Information about the inorganic parts of the composites can be obtained by measuring ^{27}Al and ^{29}Si NMR. For organosilicate species with a direct Si–C bond, the coordination of the silicon atom is described by the notation T^n

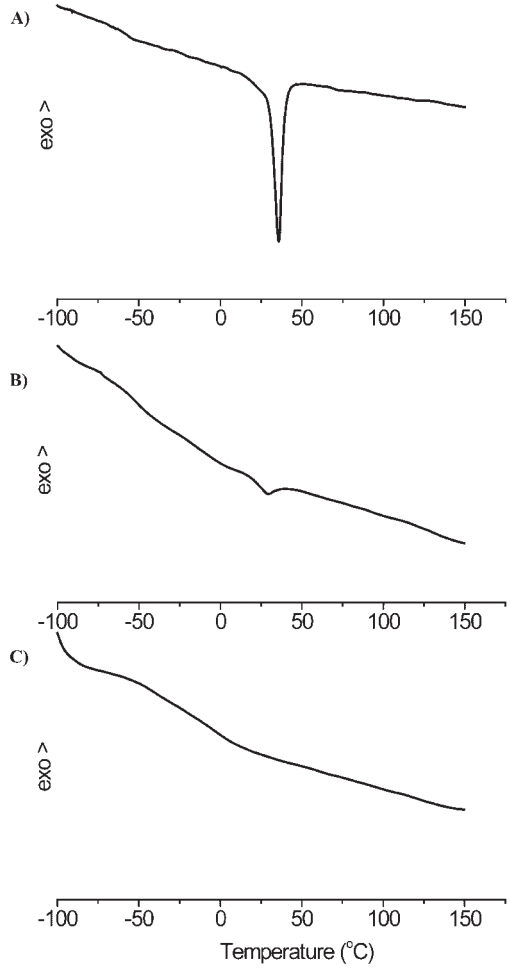

Figure 4. DSC measurements A) PEO-*b*-PHMA block copolymer, T273, along with synthesized hybrid materials with B) 21 wt.-% and C) 38 wt.-% metal alkoxides in the hybrid materials.

($n = 0, 1, 2$ or 3), where n is the number of bridging Si–O–Si or Si–O–Al oxygen atoms (Figure 6). Different T^n species resonate at different ppm values in a ^{29}Si NMR spectrum.[19]

Figure 7 shows the ^{1}H-^{29}Si CP-MAS spectra of the spherical (T273/1), hexagonal (T273/2), and lamellar (T273/3) composites. In all three spectra, peaks arising from T^1, T^2, and T^3 sites can be clearly distinguished. Most of the silicon atoms are connected to two or three other metal atoms (silicon or aluminium) by oxygen bridges, thereby yielding a three-dimensional network. The populations of the various silicon environments do not significantly change as a function of composite morphology. It seems that the observed differences more likely reflect normal fluctuations in the metal alkoxide hydrolysis step.

Single pulse ^{27}Al MAS NMR was performed to determine what kind of aluminium species are present in the composites. Figure 8 shows the ^{27}Al spectra of the same three hybrids, whose ^{29}Si spectra were compared in Figure 7. Two peaks are visible, one due to octahedrally coordinated aluminium at 6.2 ppm and one due to tetrahedrally coordinated aluminium at 56.5 ppm. The tetrahedrally coordinated aluminium can be assumed to be incorporated into the aluminosilicate lattice, whereas the octahedrally coordinated aluminium is attributed to aluminiumoxohydroxo complexes.[8] More than 50% of the aluminium is incorporated into the network as a fourfold coordinated species. Significantly, no peak is present in the 30–40 ppm region, which is where highly distorted tetrahedral sites would be expected to resonate. This indicates that there is not a significant number of severely distorted aluminium sites in the aluminosilicate network. The relative intensities of the sites vary slightly from sample to sample, but no systematic relation to hybrid morphology was observed.

The results obtained by solid-state NMR suggest that the polymer does not play a significant role in the inorganic network formation since the relative populations of the different silicon T-sites in the present composites do not differ from those found in hybrids derived from the pure hydrolyzed GLYMO/aluminium-*sec*-butoxide mixture.[8] Furthermore, the NMR spectra are similar to those obtained from hybrid materials synthesized with the structure-directing agent, PI-*b*-PEO.[20] This establishes that, as expected, the hydrophobic block, which does not directly interact with the metal oxides, has little effect on their microstructure.

Nano-Objects

For PI-*b*-PEO derived hybrid materials rich in PI, it has been shown that they can be utilized to obtain well-defined nanoparticles of different shapes.[21] This is possible since the condensation of the metal alkoxides leads to a covalent three-dimensional network incorporating the PEO block of the PI-*b*-PEO block copolymer, as demonstrated by solid-state NMR.[19,20] Thus, selective swelling of the purely organic PI phase ultimately leads to single, isolated hybrid objects of controlled shape and size. These nanoparticles have potential applications, e.g., as fluorescent markers in the area of nanobiotechnology. Figure 9 and 10 show the TEM and AFM images, respectively, of nanoparticles prepared from the present PEO-*b*-PHMA/aluminosilicate nanocomposites. These images demonstrate that dissolution of the bulk phases leads to nanoparticles with sphere, cylinder and plate shapes. It is interesting to note that after dissolution in the organic solvent, the particles are expected to be covered by a thin layer of the hydrophobic block, PHMA, in analogy to what was found for PI-*b*-PEO hybrids.[21] Since the nanoparticles can themselves be used as fillers to generate nanocomposites,[22] by changing the hydrophobic block of the structure-directing block copolymer, nanoparticles compatible with different synthetic polymers can be derived.

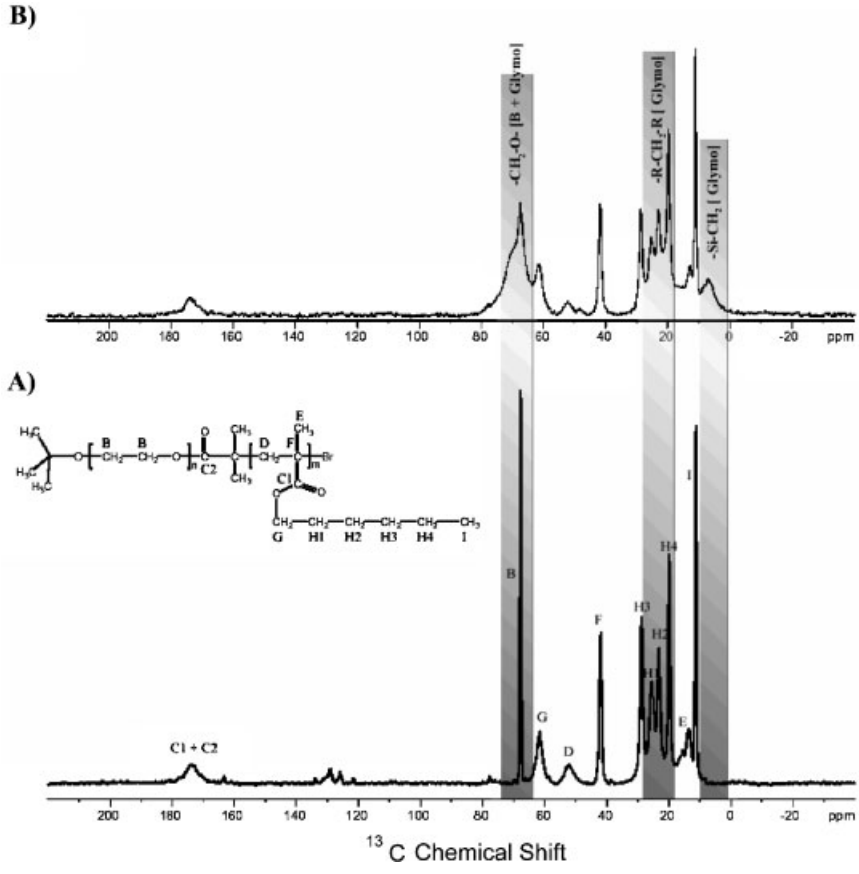

Figure 5. ^{1}H-^{13}C CP-MAS spectra A) PEO-*b*-PHMA block copolymer (T273) and B) composite material with lamellar morphology (52 wt.-% metal-alkoxides). Reference: $Si[Si(CH_3)_3]_4 = 0$ ppm.

Mesoporous Materials

Finally, block copolymer directed composites for which the organic-inorganic network forms the matrix can be used to prepare mesoporous materials with controlled pore sizes. One of the composite materials, T55/1, exhibits an inverse hexagonal morphology of PHMA cylinders in a PEO/aluminosilicate matrix. For such structures, heat treatment at elevated temperatures is expected to lead to mesoporous materials with accessible pores as shown in Figure 1. A representative SAXS pattern of composite T55/1 after calcination in several stages up to 600 °C is shown in Figure 11A. The data reveals higher order reflections consistent with a hexagonal order. This result is confirmed by the TEM image of the same sample depicted in Figure 11B, clearly demonstrating that the hexagonal symmetry of the sample is retained. From the TEM data, the average distance between the centers of two cylinders is about 16.7 nm, which is in good agreement with the SAXS result of 16.1 nm.

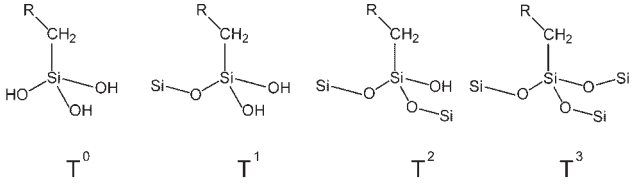

Figure 6. Representation of the T^n nomenclature of organosilicates.

Conclusions

In this study, we were able to show that the amphiphilic block copolymer PEO-*b*-PHMA can be used as an effective structure-directing agent in the synthesis of structured, organic-inorganic hybrid materials from organic, volatile solvents. So far, four different morphologies could be identified by a combination of SAXS and TEM, namely spherical, hexagonal, lamellae and inverse hexagonal. The local structure of the composites was elucidated by DSC and solid-state NMR measurements indicating that it is similar to previously studied composites using PI-*b*-PEO as

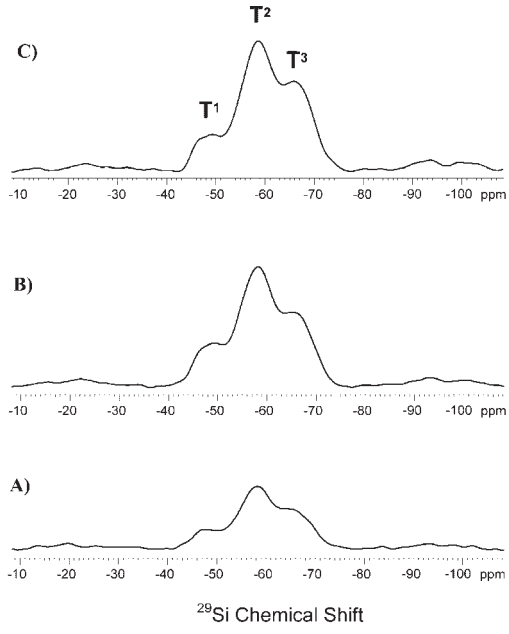

Figure 7. ^{1}H-^{29}Si CP-MAS spectra of different hybrid materials with A) spherical morphology B) cylindrical morphology and C) lamellar morphology. Reference: $Si[\underline{Si}(CH_3)_3]_4 = -9.8$ ppm.

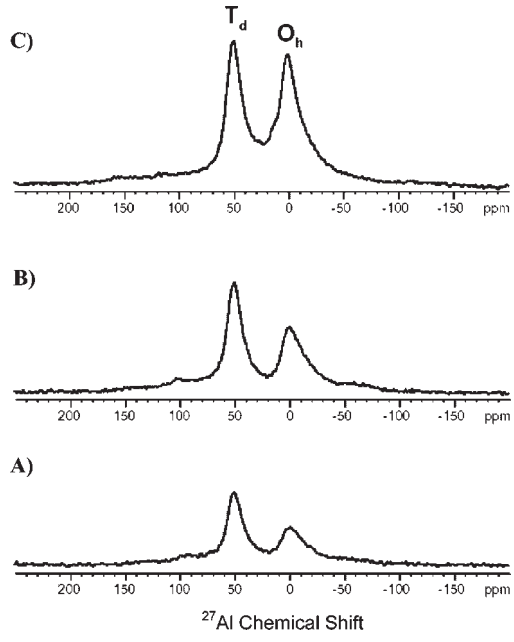

Figure 8. ^{27}Al MAS spectra of composites with A) spherical, B) cylindrical and C) lamellar morphology exhibiting tetrahedral (T_d) and octahedral (O_h) coordination of aluminium. Reference: $AlCl_3 = 0$ ppm.

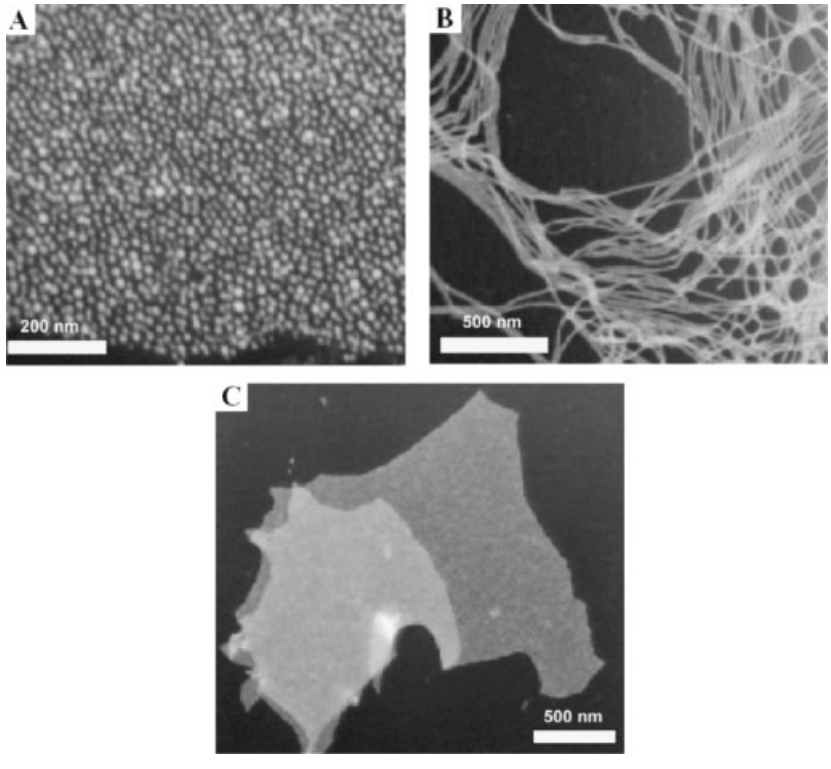

Figure 9. Dark field TEM micrographs of nano-objects obtained through dissolution of composite A) T273/1; spheres (21 wt.-% metal alkoxides) B) T273/2; cylinders (38 wt.-% metal alkoxides) and C) T273/3; plates (52 wt.-% metal alkoxides).

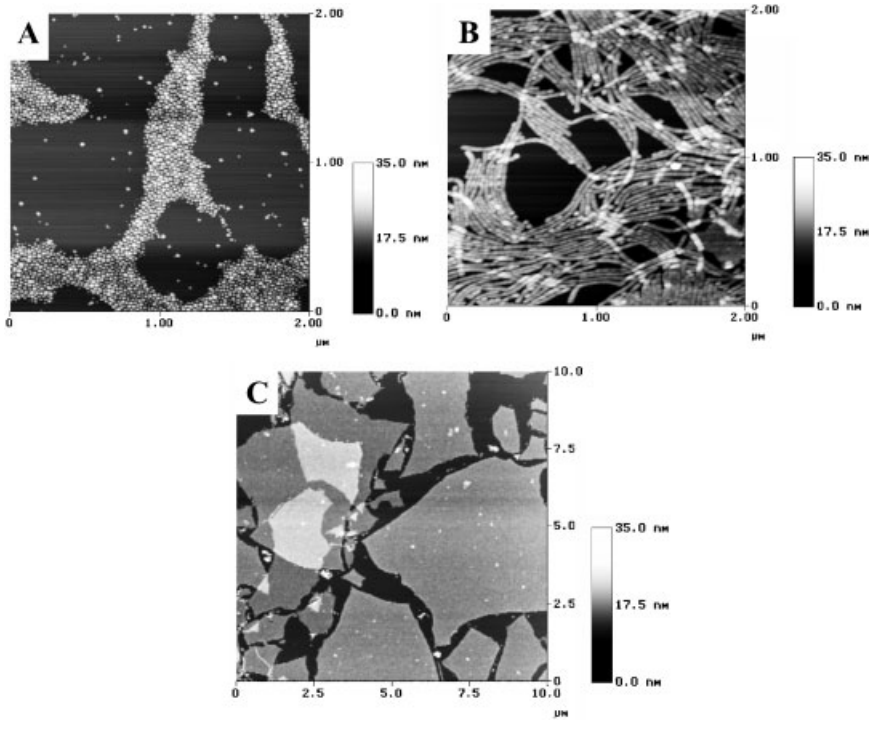

Figure 10. AFM images of calcined nano-objects A) T37/7; spheres (21 wt.-% metal alkoxides), B) T37/1; cylinders (34 wt.-% metal alkoxides) and C) T37/8; plates (53 wt.-% metal alkoxides).

structure-directing agent. Single ''hairy'' nanoparticles were obtained by dissolving hybrid materials with PHMA as the major phase in an organic solvent. With TEM and AFM, individual spheres, cylinders and lamellae were identified. The demonstration that the chemical nature of the polymer hairs covering these particles can be varied by choosing different hydrophobic blocks, opens novel approaches towards tailoring the filler-matrix interactions in model nanocomposites.[21] A mesoporous material was fabricated through heat treatment of a composite with inverse hexagonal morphology with PHMA as the minority phase. These investigations demonstrate that the present approach towards nanostructured polymer-inorganic hybrids using amphiphilic, low T_g block copolymers and cast from organic, volatile solvents can be transferred to other polymer systems beyond PI-*b*-PEO. It may access tri- und multiblock copolymers containing PI, PEO, and PHMA in some sequence, which are expected to exhibit a much richer

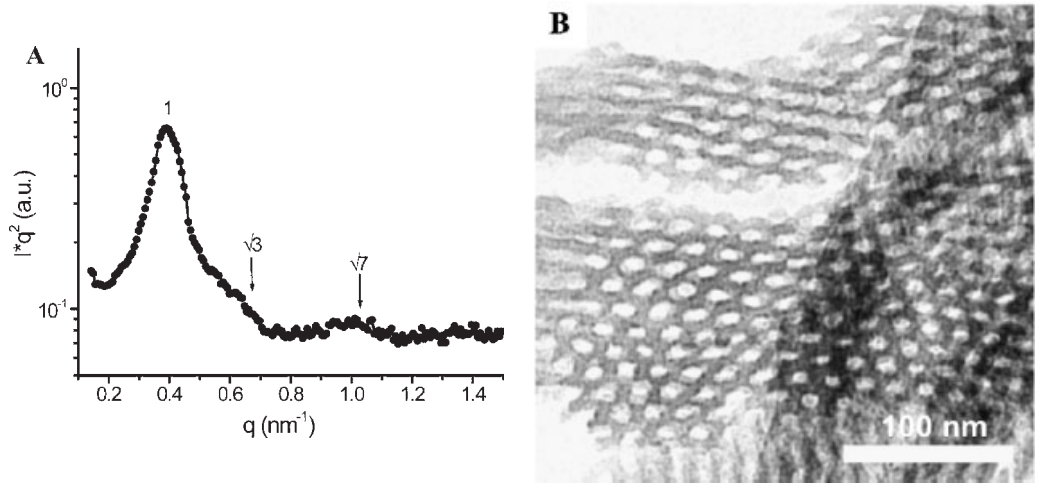

Figure 11. A) SAXS diffractogram and B) bright field TEM micrograph of composite T55/1 with inverse hexagonal morphology after calcination.

phase diagram. Studies along these lines are now in progress in our laboratories.

Acknowledgement: The financial support of the *National Science Foundation* single investigator grant (DMR-0312913) is gratefully acknowledged. The work was further supported by the *Cornell Center for Materials Research* (CCMR), a Materials Research Science and Engineering Center of the *National Science Foundation* (DMR-0079992). In particular, we thank the *CCMR's X-Ray Diffraction, Electron and Optical Microscopy* and *Hudson Mesoscale Processing* facilities. X-ray diffraction in SMG's laboratory is supported by *Department of Energy* grant DE-FG02-97ER62443.

[1] M. Templin, A. Franck, A. D. Chesne, H. Leist, Y. Zhang, R. Ulrich, V. Schädler, U. Wiesner, *Science* **1997**, *278*, 1795.
[2] S. Yang, H. Yoichi, C.-H. Chen, M. Peter, T. Thomas, *Polym. Prepr. (Am. Chem. Soc., Div. Polym. Chem.)* **2002**, *43(2)*, 386.
[3] C. G. Göltner, S. Henke, M. C. Weissenberger, M. Antonietti, *Angew. Chem. Int. Ed.* **1998**, *37*, 613.
[4] K. Yu, A. J. Hurd, A. Eisenberg, C. J. Brinker, *Langmuir* **2001**, *17*, 7961.
[5] D. Zhao, J. Feng, Q. Huo, N. Melosh, G. H. Fredrickson, B. F. Chmelka, G. D. Stucky, *Science* **1998**, *279*, 548.
[6] S. A. Bagshaw, E. Prouzet, T. J. Pinnavaia, *Science* **1995**, *269*, 1242.
[7] P. F. W. Simon, R. Ulrich, H. W. Spiess, U. Wiesner, *Chem. Mater.* **2001**, *13*, 3464, and references therein.
[8] M. Templin, U. Wiesner, H. W. Spiess, *Adv. Mater.* **1997**, *9*, 814.
[9] A. C. Finnefrock, R. Ulrich, A. D. Chesne, C. C. Honeker, K. Schumacher, K. K. Unger, S. M. Gruner, U. Wiesner, *Angew. Chem. Int. Ed.* **2001**, *40*, 1207.
[10] A. C. Finnefrock, R. Ulrich, G. E. S. Toombes, S. M. Gruner, U. Wiesner, *J. Am. Chem. Soc.* **2003**, *125*, 13084.
[11] G. Floudas, B. Vazaiou, F. Schipper, R. Ulrich, U. Wiesner, H. Iatrou, N. Hadjichristidis, *Macromolecules* **2001**, *34*, 2947.
[12] C. Auschra, R. Stadler, *Macromolecules* **1993**, *26*, 2171.
[13] R. Stadler, C. Auschra, J. Beckmann, U. Krappe, I. Voigt-Martin, L. Leibler, *Macromolecules* **1996**, *28*, 3080.
[14] W. Zheng, Z. G. Wang, *Macromolecules* **1995**, *28*, 7215.
[15] F. S. Bates, G. H. Fredrickson, *Phys. Today* **1999**, 32.
[16] T. S. Bailey, C. M. Hardy, T. H. Epps, III, F. S. Bates, *Macromolecules* **2002**, *35*, 7007.
[17] S. Mahajan, S. Renker, P. F. W. Simon, J. S. Gutmann, A. Jain, S. M. Gruner, L. J. Fetters, G. W. Coates, U. Wiesner, *Macromol. Chem. Phys.* **2003**, *204*, 1047.
[18] M. W. Tate, S. M. Gruner, E. F. Eikenberry, *Rev. Sci. Instrum.* **1997**, *68*, 47.
[19] S. Mann, S. L. Burkett, S. A. Davis, C. E. Fowler, N. H. Menelson, S. D. Sims, D. Walsh, N. T. Whilton, *Chem. Mater.* **1997**, *9*, 2300.
[20] D. M. De Paul, J. W. Zwanziger, R. Ulrich, U. Wiesner, H. W. Spiess, *J. Am. Chem. Soc.* **1999**, *121*, 5727.
[21] R. Ulrich, A. D. Chesne, M. Templin, U. Wiesner, *Adv. Mater.* **1999**, *11*, 141.
[22] A. Jain, J. S. Gutmann, C. B. W. Garcia, Y. Zhang, M. W. Tate, S. M. Gruner, U. Wiesner, *Macromolecules* **2002**, *35*, 48.

